PROCEEDINGS, Twelfth Workshop on Geothermal Reservoir Engineering
Stanford University, Stanford, California, January 20-22, 1987
SGP-TR-109

PETROPHYSICAL PROPERTIES OF TWENTY DRILL CORES FROM THE LOS AZUFRES, MEXICO, GEOTHERMAL FIELD

E. R. Iglesias, E. Contreras L., A. García G.
Instituto de Investigaciones Eléctricas
Apartado Postal 475
Cuernavaca, Morelos 62000, México

Bernardo Domínguez A.
Comisión Federal de Electricidad
Av. Las Camelinas 3527, 10^{o} P.
Morelia, Michoacán, México

ABSTRACT

For this study we selected 20 drill cores covering a wide range of depths (400-3000 m), from 15 wells, that provide a reasonable coverage of the field. Only andesite, the largely predominant rock type in the field, was included in this sample. We measured bulk density, grain (solids) density, effective porosity and (matrix) permeability on a considerable number of specimens taken from the cores; and inferred the corresponding total porosity and fraction of interconnected total porosity. We characterized the statistical distributions of the measured and inferred variables. The distributions of bulk density and grain density resulted approximately normal; the distributions of effective porosity, total porosity and fraction of total porosity turned out to be bimodal; the permeability distribution resulted highly skewed towards very small (1 mdarcy) values, though values as high as 400 mdarcies were measured. We also characterized the internal inhomogeneity of the cores by means of the ratio (standard deviation/mean) corresponding to the bulk density in each core (in average there are 9 specimens per core). The cores were found to present clearly discernible inhomogeneity; this quantitative characterization will help design new experimental work and interpret currently available and forthcoming results. We also found statistically significant linear correlations between total density and density of solids, effective porosity and total density, total porosity and total density, fraction of interconnected total porosity and the inverse of the effective porosity, total porosity and effective porosity; bulk density and total porosity also correlate with elevation. These results provide the first sizable and statistically detailed database available on petrophysical properties of the Los Azufres andesites.

INTRODUCTION

Prior to this work, little information existed about petrophysical properties of rocks from the Los Azufres geothermal field. This paucity of information adversely affected several important geothermal engineering activities related to the field, such as reserve and producibility assesment, design of drilling bottomhole assemblies, and design and interpretation of stimulation and reinjection operations. In this paper we present a relatively extensive original set of petrophysical data and correlations pertaining to andesite rock from the field. The scope of this work has been outlined in the Abstract and will not be repeated. It is worth noting however, that the results presented here are only the first part of a significantly greater effort that will also include mechanical, thermal and petrological properties of these cores.

Previous work on the subject reduces to that of Iglesias et al. (1985), and Contreras et al. (1986). In the 1985 paper we presented results on bulk and grain density, effective porosity, permeability, mechanical properties and thermal properties of Los Azufres andesites from 5 different outcrops. In the other paper we also dealt with a limited amount of material (samples from 8 outcrops, and a total of 4 drill cores, from wells Az-1, Az-5, Az-9 and Az-19). In this case we measured 10 different properties, though most of them on a very limited amount of samples: bulk density and effective porosity (all outcrops and cores), permeability (cores Az-5, Az-9 and Az-19), bulk compresibility (one outcrop and cores Az-9 and Az-19), compressional and shear wave velocities (one outcrop), electrical resistivity (one outcrop), thermal conductivity (core Az-19), thermal diffusivity (core Az-19), and thermal expansion (one outcrop). The present work is significantly more extensive and in-depth, presenting statistically characterized results of 7 properties (see Abstract) corresponding to 20 new cores from 15 wells.

MATERIALS AND METHODS

The cores for this study were selected according to availability, type of rock (only andesite, the largely predominat type in the field was included), and degree of hidrothermal alteration (efforts were made to try and include samples covering the whole range of alteration).

Fig. 1 presents the areal distribution of the cores in the field, which shows a reasonable coverage. Table 1 summarizes other characteristics of the cores. The percentage of hydrothermal alteration quoted is actually the average hydrothermal alteration in a 40 m interval straddling the depth of the core, and was obtained by thin section

Table 1. Characteristics of drill cores used in this study

Well	Core	Hydrothermal alteration (%)	Number of specimens (#)
Az-3	1	90	16
Az-3	4	85	14
Az-3	5	90	9
Az-4	3	95	14
Az-5	1	30	8
Az-8	2	80	9
Az-10	1	75	10
Az-20	1	50	10
Az-20	3	70	8
Az-22	2	85	9
Az-25	1	84	11
Az-26	2	80	6
Az-26	3	85	8
Az-29	1	71	10
Az-29	3	45	6
Az-41	2	77	8
Az-46	3	90	6
Az-47	4	95	8
Az-48	4	N.A.	5
Az-50	3	27	5

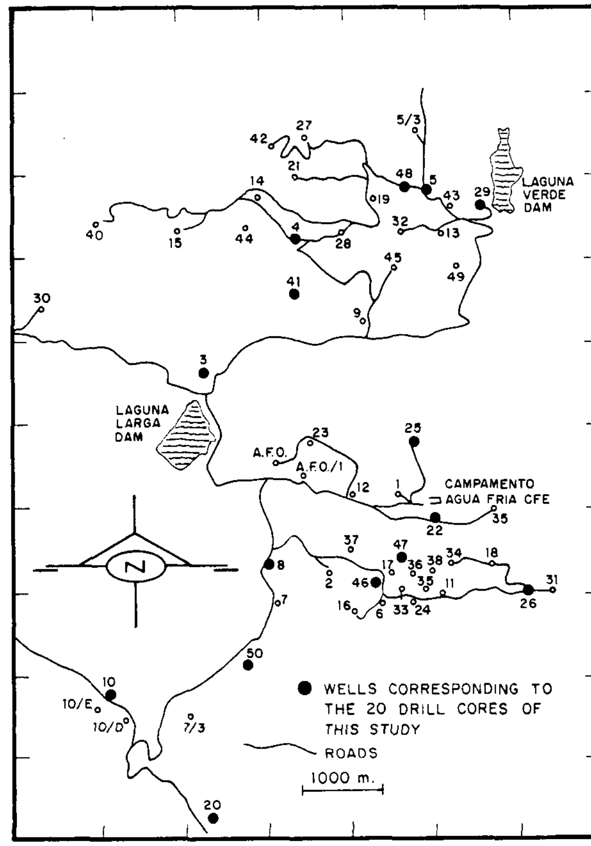

Fig. 1 Areal distribution of the cores in the field.

petrographic studies of drill cuttings (Martiñón-García, 1986); thus, this parameter must be taken only as possibly indicative of the alteration of the cores. Detailed petrographic studies of the cores are currently underway.

The altitude distribution (Fig. 2) is skewed towards shallow cores, and there are no samples in the 1100-1500 m a.s.l. interval. It is hoped that more cores will be available in the future to improve the representativity of the sample.

Bulk and grain density, and effective porosity were measured by methods recommended by the International Society for Rock Mechanics (ISRM, 1972). Permeability was measured with a Core Lab gas permeameter; dry air and nitrogen were used as fluids; results were corrected for slippage (Klinkenberg effect). Bulk density was measured in 180 specimens, and effective porosity was measured in 179 specimens from the 20 cores (e.g., Table 1); permeability was measured in 50 specimens from 17 cores, due to availability. Grain density,

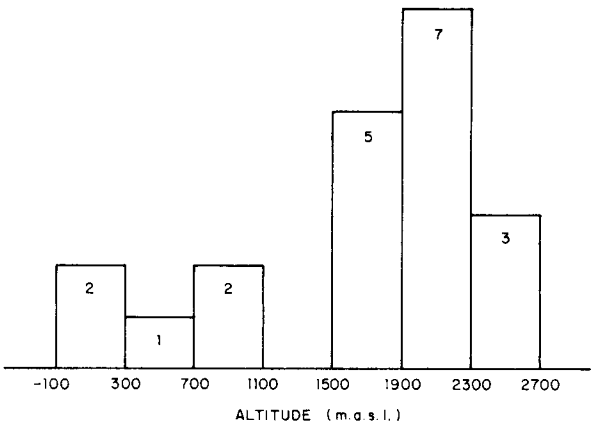

Fig. 2 Altitude distribution of the cores.

approximately averaged over each core, was measured on rock powder obtained by grinding several leftover pieces of core (typically 300 g). Mean total porosity for each core was inferred from the corresponding average bulk and grain density. The mean fraction of interconnected porosity for each core was inferred from the corresponding average effective and total porosity.

The raw data suggested a significant degree of internal inhomogeneity in some of the cores. Thus, we set off to quantitatively characterize the inhomogeneity. We considered the bulk density and effective porosity results obtained for each core. The existence of about 9 specimes, in average, per core, provided mean values and standard deviations of these properties for each core. To characterize the inhomogeneity we examined the ratios of the standard deviation to the corresponding mean, for both properties. To avoid any possible dependence of the accuracy of the measurements on the magnitude of the measured property, we tested the data for the existence of correlations between standard deviations and the corresponding means. We found that, unlike effective porosity, bulk density did not reveal such correlation, and therefore can confidently be used to characterize the inhomogeneity of the cores.

RESULTS AND DISCUSION

Fig. 3 displays the distribution of the grain density, averaged over each core, for the 20 cores. The corresponding mean and standard deviation are 2.799 and 0.092 g cm^{-3} respectively. Very nearly 50% of the population lies at each side of the mean, suggesting a normal distribution.

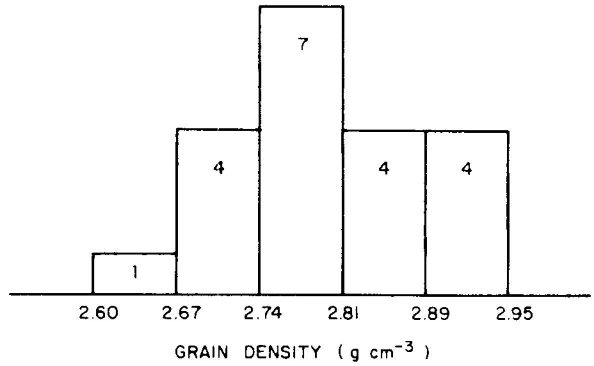

Fig. 3 Distribution of grain density.

Fig. 4 presents the distribution of bulk density, as inferred from 180 specimens from the 20 cores. The corresponding mean and standard deviation are 2.468 and 0.225 g cm^{-3} respectively. In this case too, nearly 50% of the population lies at each side of the mean, suggesting a normal distribution.

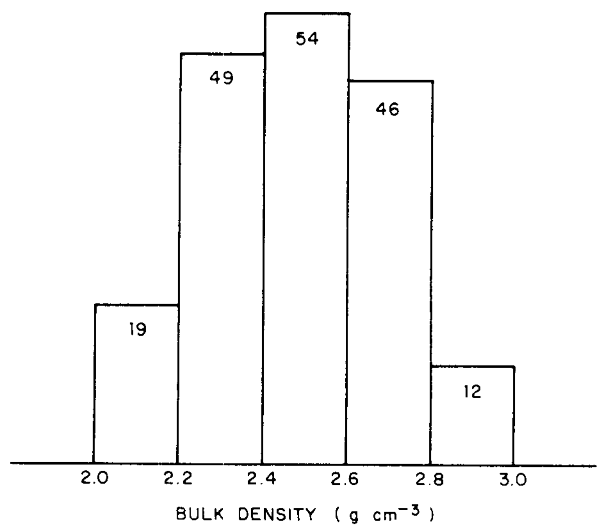

Fig. 4 Distribution of bulk density.

The histogram of Fig. 5 (179 specimens, 20 cores) suggests a bimodal distribution for effective porosity, with a lower mode of approximately 2%, and an upper mode of approximately 14%. Note that more than 32% of the sample presents effective porosity values greater than or equal to 14%, which could be regarded as atypically high for andesites. We suspect that the high-porosity peak is associated with hydrothermal alteration while the low-porosity peak reflects unaltered rock; confirmation of this speculation is contingent upon completion of the ongoing petrographic studies.

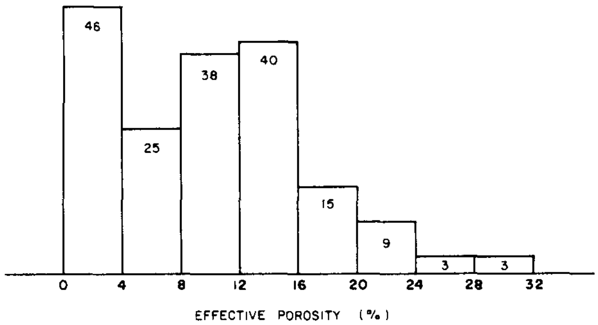

Fig. 5 Distribution of effective porosity.

Fig. 6 ilustrates the permeability distribution [50 specimens, 17 cores, no measurements were possible for cores Az-29(3), Az-46(3) and Az-48(4)]. Note that the vertical scale is logarithmic. About 80% of the sample has permeability values of less than 2.3 mdarcy, which may be regarded as consistent for these tight igneous rocks; the rest lies in the range 2.3-400 mdarcy. None of the specimens showed microfractures perceptible to the naked eye; thus, we speculate that the high permeability tail might be related to hidrothermal alteration. Again, confirmation of this possibility is contingent upon completion of ongoing petrographic studies. The present results, which reflect matrix (as opposed to fracture) permeability, are consistent with previous findings (Iglesias et al., 1985; Contreras et al. 1986).

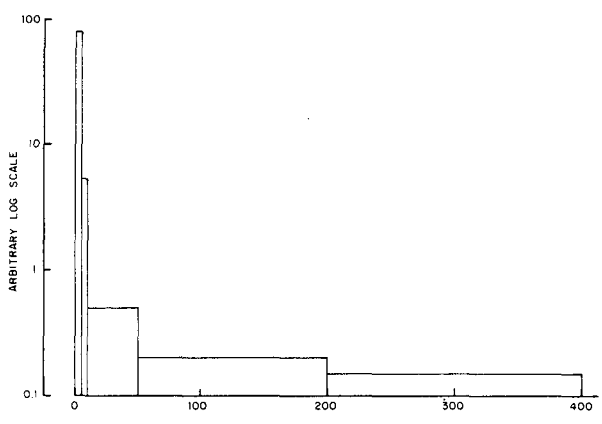

Fig. 6 Distribution of (matrix) permeability.

The inferred distribution for total porosity (average per core) looks bimodal (Fig. 7), with a lower mode of approximately 6%, and an upper mode of approximately 14%. Not surprisingly, the bimodality of this distribution corresponds to that of the effective porosity. The discrepancy between the values of the lower modes of both porosity distributions is an artifact of the differing sizes (n=179 for effective porosity, n=20 for total porosity) of the samples involved. In fact, the discrepancy disappears if average effective porosity per core is used instead of the 179 measured values.

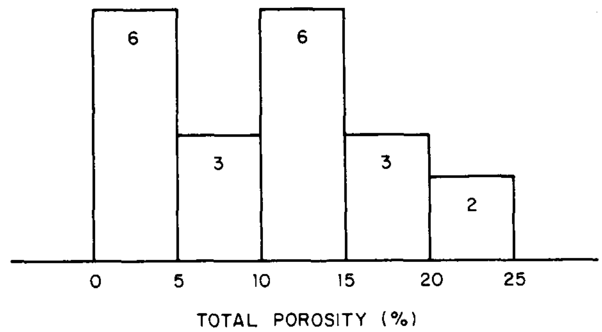

Fig. 7 Distribution of total porosity.

The histogram of Fig. 8 suggests a bimodal distribution for the inferred fraction of interconnected total porosity, with a lower mode of about 0.3, and an upper mode of about 0.9. Interestingly, roughly 70% of the sample displays high (>0.8) connectivity.

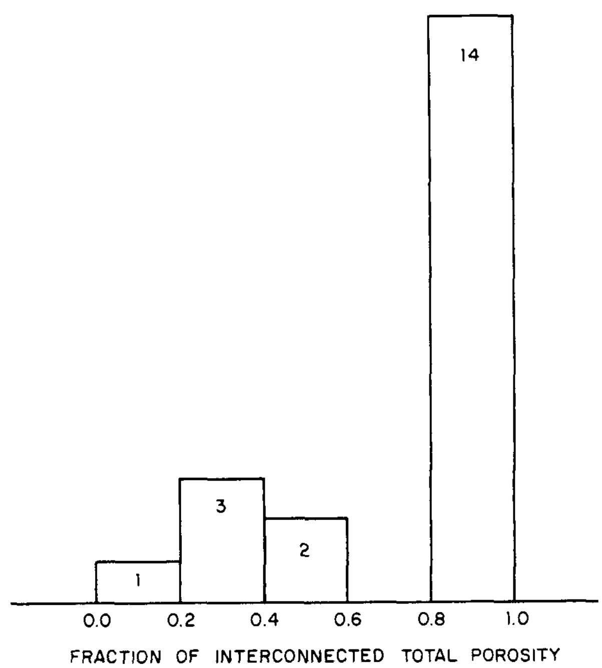

Fig. 8 Distribution of fraction of interconnected total porosity.

The distribution of the heterogeneity ratio (from bulk density) illustrated in Fig. 9., is skewed to the left, with a mode approximately equal to 0.0090, and mean and standard deviation equal to 0.0149 and 0.0085 respectively. Thus, the cores examined present a relatively moderate, but clearly discernible inhomogeneity. An inmediate application of these results was to provide a quantitative criterium for deciding how many thin sections should be studied for each core, for petrographic characterization. These results also help to understand the variability found in the correlations that follow.

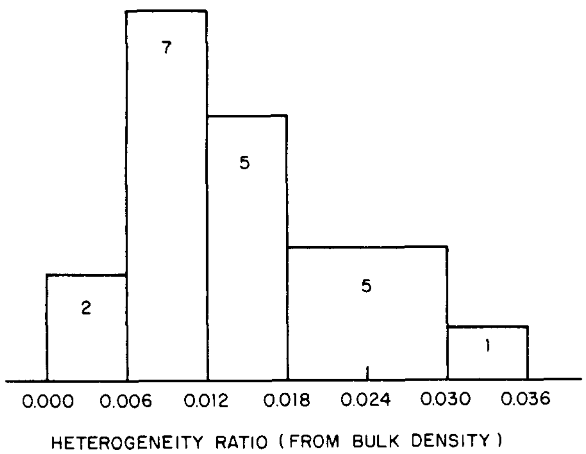

Fig. 9 Distribution of heterogeneity ratio.

Several interesting linear correlations, all of them statistically significant at the 99.5% confidence level, were found among these physical properties. A relatively loose correlation is present between bulk density and grain density (Fig. 10). Thus, the data indicates that approximately $100r^2=45\%$ of the variability of r_B is due to r_G.

A tight correlation exists between effective porosity and bulk density (Fig. 11).

The fraction of interconnected total porosity also correlates with bulk density (Fig. 12), though the correlation is weaker than that of effective porosity.

Total porosity correlates very tightly with effective porosity (Fig. 13).

The fraction of interconnected total porosity correlates with the inverse of

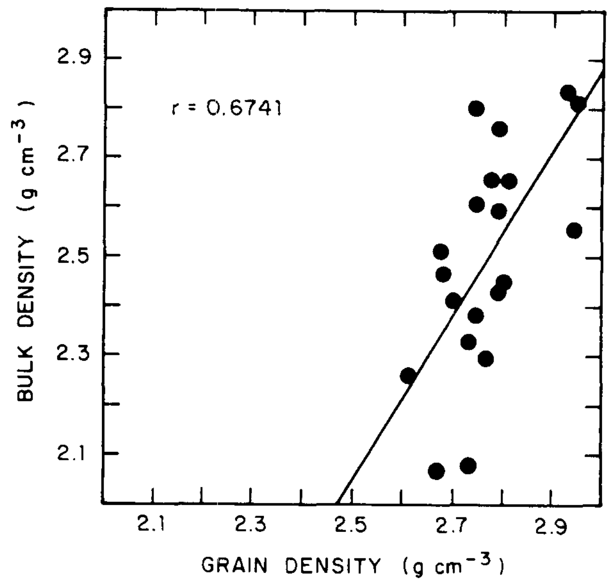

Fig. 10 Correlation between bulk and grain density.

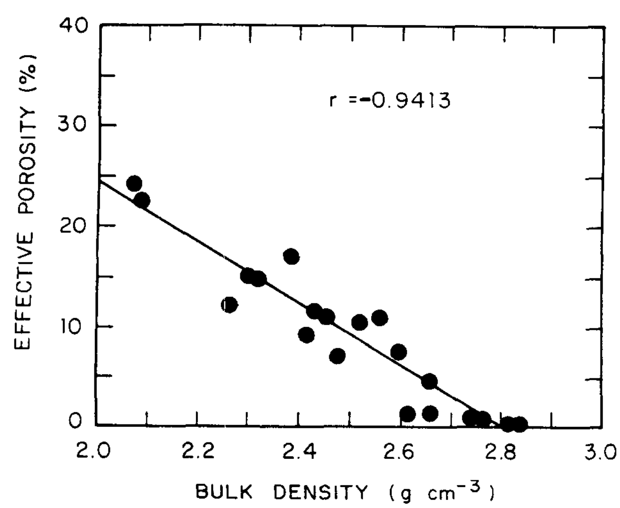

Fig. 11 Correlation between effective porosity and bulk density.

the effective porosity (Fig. 14). The bimodal character of the fraction of interconnected total porosity is evident in the graph.

Finally, both bulk density and total porosity correlate with altitude (Figs. 15 and 16 respectively), reflecting lithostatic load.

The present results are extremely useful for several important geothermal engineering activities related to the field, such as reserve and producibility assesment, design of drilling bottomhole assemblies, and design and interpretation of stimulation and reinjection operations.

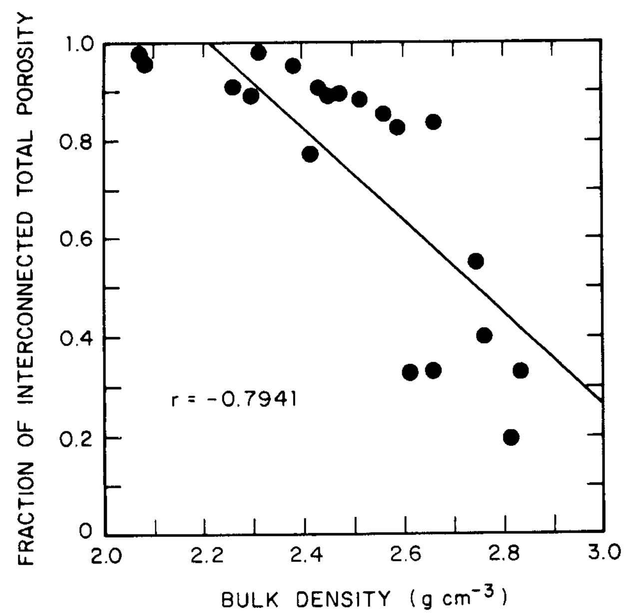

Fig. 12 Correlation between fraction of interconnected total porosity and bulk density.

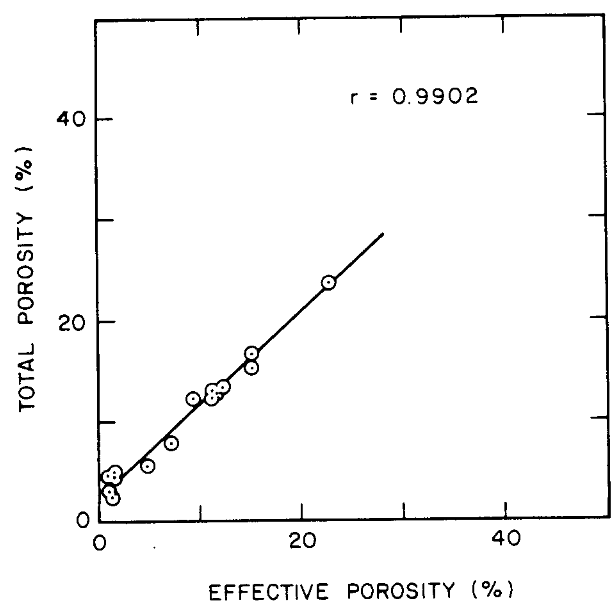

Fig. 13 Correlation between total and effective porosity.

REFERENCES

Contreras E., Iglesias E.R. and Razo A., 1986 "Initial measurements of petrophysical properties on rocks from the Los Azufres, Mexico, geothermal field", Proc. 11th. Workshop Geothermal Reservoir Engineering, pp. 51-57, Stanford University, SGP-TR-93.

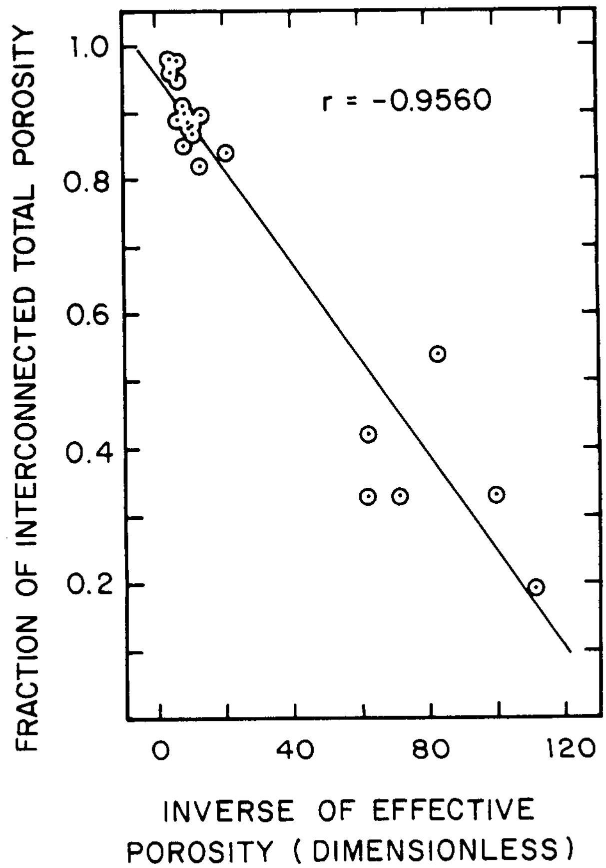

Fig. 14 Correlation between fraction of interconnected total porosity and inverse of effective porosity.

Iglesias E.R., Contreras E. and García A., 1985 "Propiedades petrofísicas de andesitas superficiales del campo geotérmico Los Azufres", Report IIE/11/2014/I 01/P, 102 pp., Instituto de Investigaciones Eléctricas.

ISRM, 1972 "Suggested methods for determining water content, porosity, density, absorption and other related properties", International Society for Rock Mechanics, Commission on Standarization of Laboratory and Field Tests, Document No. 2, Lisbon, Portugal.

Martiñón-García H., 1986 "Porcentajes de alteración en núcleos de pozos de Los Azufres, Michoacán", Comunicación de Geología 11/86, 4 pp., Gerencia de Proyectos Geotermoeléctricos, Comisión Federal de Electricidad.

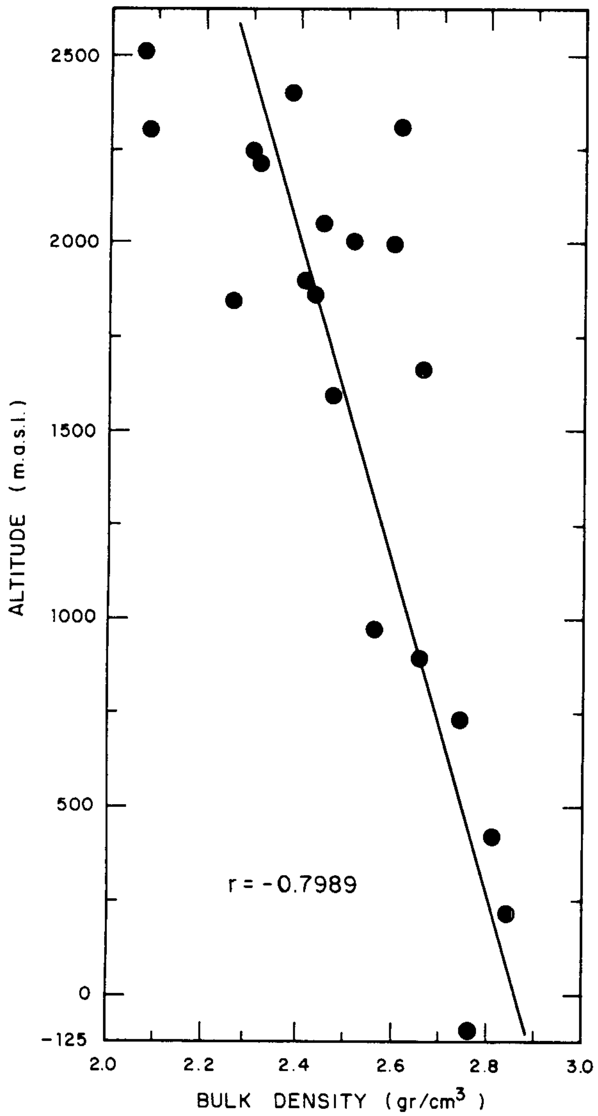

Fig. 15 Correlation between bulk density and altitude.

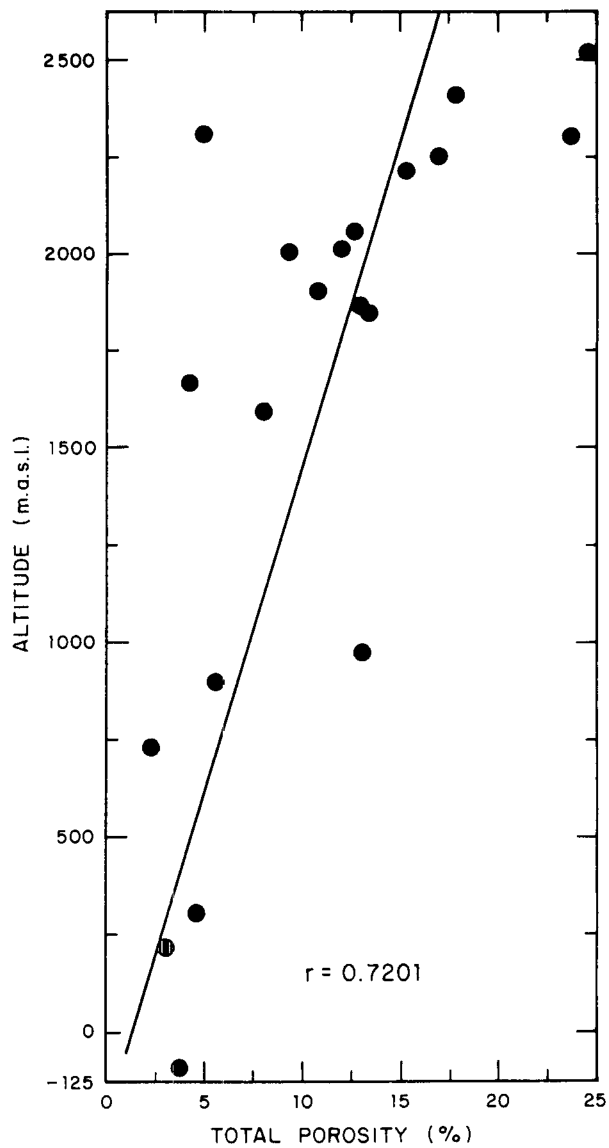

Fig. 16 Correlation between total porosity and altitude.